

Yield Property Characterization for Au and TiN Thin Films by Applying Nanoindentation Technique

Yun-Hee Lee^{1, a}, Yong-Hak Huh^{1, b}, Ju-Young Kim^{2, c},
Seung-Hoon Nahm^{1, d}, Jae-il Jang^{3, e} and Dongil Kwon^{2, f}

¹Center for Environment and Safety Measurement, Korea Research Institute of Standards and Science, Daejeon 305-340, Korea

²School of Materials Science and Engineering, Seoul National University, Seoul 151-742, Korea

³Department of Materials Science and Engineering, Hanyang University, Seoul 133-791, Korea

^auni44@kriss.re.kr, ^byhhuh@kriss.re.kr, ^cjuyoung1@snu.ac.kr, ^dshnahm@kriss.re.kr,
^ejjjang@hanyang.ac.kr, ^fdongilk@snu.ac.kr

Keywords: Thin film, Yield strength, Nanoindentation, 3D indent visualization.

Abstract. We tried to apply the nanoindentation technique to yield strength characterization by modifying a previous research. Although the yield strength determining technique developed by Kramer et al. has been successfully demonstrated for large scale indentations on bulky metals, its applicability is still doubtful to nanoscale indentations on thin films with severe roughness, anisotropy, and interfacial constraint. In order to overcome these problems, we combined the nanoindentation technique with a three-dimensional indent visualization technique in this study. Nanoindentation tests were performed for Au and TiN thin films and their corresponding indents were scanned by using an atomic force microscope. From the three-dimensional pile-up morphology, a circular pile-up boundary was measured and input into the yield strength formulation as an effective yielded zone radius. The yield strengths calculated were directly compared with those from the microtensile test.

Introduction

Nanoindentation measuring applied load and indenter penetration depth during a contact deformation is one of the most powerful techniques for evaluating the mechanical properties of thin films [1]. This technique has not only the merits of conventional hardness measurement such as testing simplicity, nondestructiveness, and economical aspect but also the merits of instrumented technique such as simultaneous testing data gathering and property analysis without additive specimen observation. Typical nanoindentation researches constrained within the determination of elastic modulus, hardness, and fracture toughness are now being expanded to the analysis of plastic flow curve, residual stress, interfacial toughness, and tribological properties [1-4].

Especially, an attempt has been made to measure and correlate the extent of nanoindentation-induced plastic zone to the yield stress of the indented material [5]. Radius of the hemispherical plastic zone was approximated as the boundary of material upheaved or pile-up region around the remnant indent and was measured by line profiling across the indent. Kramer et al. [5] derived Eq. (1) based on Johnson's analysis [6] of a spherical cavity under indentation to relate yields strength to the plastic zone radius.

$$\sigma_y = \frac{3L_{\max}}{2\pi c^2} \quad (1)$$

where L_{\max} is the peak indentation load and σ_y is the yield strength of the indented material. Although this model assumes that the tested material is isotropic, homogeneous, and undergoes no strain hardening [5,6], actual thin films having significant texture microstructure, roughness,

residual stress and substrate effect can result in anisotropic pile-up pattern and thus the previous line profiling method cannot describe detailed shape and dimension of the plastic zone.

In this paper, we combined direct imaging and three-dimensional visualization technique for the resulting indent morphology. Different with the line profile results, the pile-up boundary was clearly determined as a closed contour on the basal plane. The yield strengths from Eq. (1) were compared with the results from concurrent microtensile testing for the same thin films. From the comparison of analyzed results, the validity of Eq. (1) for the nanoscale indentations on thin films was discussed and related discrepancy was explained from the particularity of thin film deformation.

Experimental procedure

1 μm -thick Au and TiN thin films deposited on silicon wafers by sputtering technique were used in this study. The yield strengths of these thin films have been already measured through microtensile tests in previous study [7]. The micro-sized free-standing film specimen was fabricated by electromachining process and deformed in a microtensile tester with microactuator and microstrain measurement units. Detailed information on the microtensile tests can be obtained from Reference [7]. Nanoindentations were performed with the MTS system using a Berkovich pyramidal indenter. A trapezoidal loading profile with maximum loads of 1, 2, 5, and 8 mN was selected for Au thin film while the loading profile with peak loads of 6 and 10 mN was used for TiN thin film. Four indentations were made at each load step. All indentation load versus depth curves were analyzed according to the Oliver and Pharr's unloading curve analysis [1] and the resulting indentations were imaged shortly after indentation with a PSIA X100 atomic force microscope. From the three-dimensional morphology information on the indented surface, the extent of plastically deformed zone was analyzed using the Matlab® visualization software.

Results and discussion

The nanoindentation curves obtained from both Au and TiN films are superposed in Fig. 1. Peak penetration depth h_{max} for Au film was about 400 nm at peak load 8 mN while that for TiN film was less than 130 nm at peak load 10 mN. Hardness and reduced modulus analyzed from the unloading parts are plotted in Fig. 2.

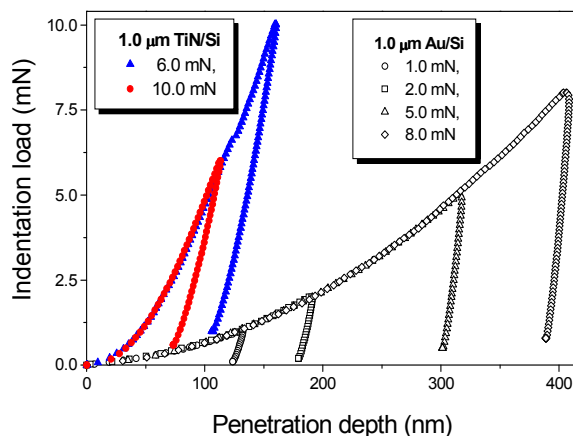


Fig. 1. Nanoindentation load-depth curves for Au and TiN thin films.

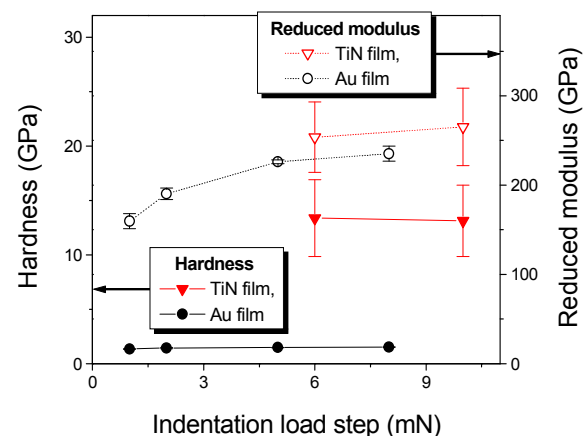


Fig. 2. Hardness and reduced modulus analyzed from nanoindentation curve

The hardness of Au thin film decreased from 1.54 ± 0.03 GPa at 8 mN to 1.35 ± 0.04 GPa at 1 mN due to the effects of interfacial constraint and hard Si substrate. In the case of TiN thin film, the hardness was 13.26 ± 3.16 GPa regardless of the peak load. The large data scatter in TiN thin film is attributed to its rough surface; average roughness measured using the atomic force microscope were 3.8 and 9.1 nm for Au and TiN thin films, respectively.

Three-dimensional data of the indented region obtained from the atomic force microscope was plotted using the Matlab® visualization software, as shown in Fig. 3. Significant material pile-up was observed around the indents on Au thin film while the indentation-induced surface upheaval was concealed by surface roughness in TiN thin film.

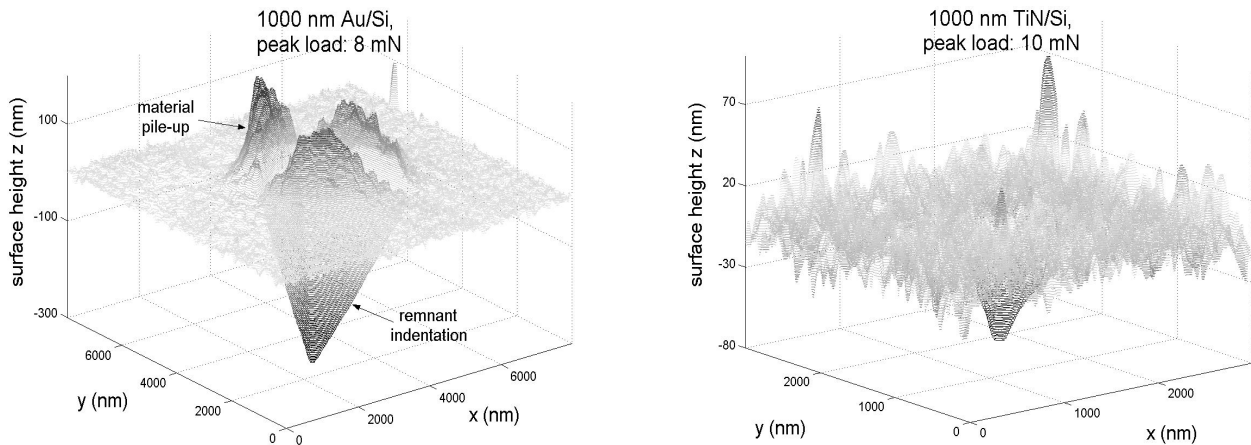


Fig. 3. Three-dimensional surface images of (a) the 8 mN indent on Au thin film and (b) the 10 mN indent on TiN thin film.

Since a determination of the effective plastic zone radius c in Eq. (1) is a key step for the yield strength calculation, we tried to analyze an exact intersecting boundary of the pile-up region and basal reference plane. An exact level of the reference plane was settled by considering the change of net volume formed by surface roughness; an arbitrary surface height corresponding to zero net volume was offset to zero level. Two-dimensional contour graph was plotted for the indented region and the surface pile-up boundary was determined from the outermost contour line in Fig. 4. The deformation area inside of the pile-up boundary was measured and converted to an effective circular plastic zone because the indentation-induced deformation zone was assumed to be a hemispherical shape with its radius c [5]. The pile-up pattern was close to a circular shape representing an isotropic deformation behavior of Au thin film.

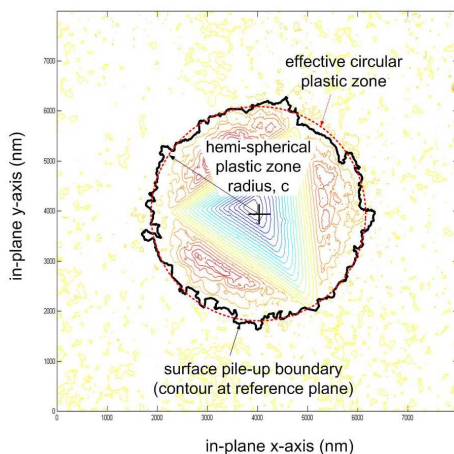


Fig. 4. Pile-up boundary determination from 2D contour of the indented surface.

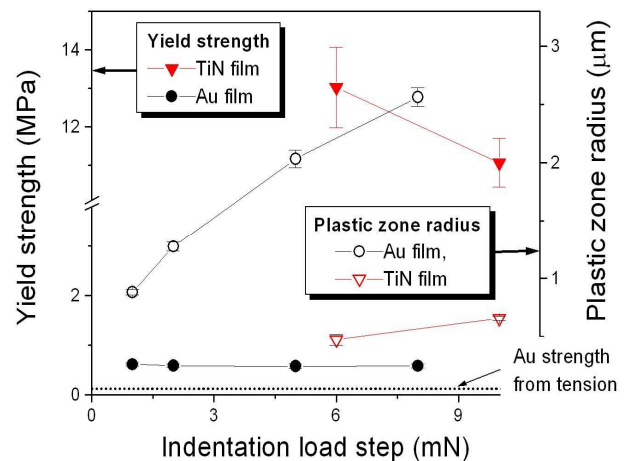


Fig. 5. Yield strength and plastic zone size estimated from the indent morphology.

The trend of plastic zone radius with indentation load in Fig. 5 was very similar with previous reports [5]. By inputting applied load and determined plastic zone radius into Eq. (1), yield strengths of Au and TiN thin films are estimated and overlapped on Fig. 5. The yield strength of Au thin film was 0.58 ± 0.04 GPa at 8 mN and nearly constant regardless of the indentation load. However, this value was about two times higher than the yield strength 0.25 ± 0.01 GPa from the

microtensile test. This difference is attributed to unexpected plastic deformation in the Au thin film; since a hard Si substrate prohibits the indentation-induced radial plastic deformation, plastic flow occurs along lateral direction parallel to the interface. Although a clear description is difficult for the nanoindentation-induced subsurface deformation, a simple disk-shaped plastic zone can be approximated for the indent on Au thin film at 8 mN instead of the hemispherical plastic zone. Thickness and radius of the disk plastic zone are assumed to be the film thickness t and measured pile-up radius c . Without considering detailed changes in radial stress state or in rigid substrate effect, the yield strength could be recalculated by considering the load supporting area $\pi c^2 + 2\pi ct$ of the disk shape instead of $2\pi c^2/3$ of the hemispherical shape. The estimated value was 0.33 ± 0.02 GPa and more comparable with yield strength from the microtensile test. Detailed shape change of the plastic zone, load supporting capacity of the substrate, and more sensitive pile-up determination for extremely low indentation load will be investigated in future study. In the case of TiN thin film, the yield strength was 11.07 ± 0.62 GPa at the indentation load 10 mN. However, the yield strength could not be measured from the microtensile test because free-standing TiN film broke without any plastic deformation. This phenomenon means that the nanoindentation can be a powerful tool for estimating deformation properties of brittle solids.

Summary

In order to estimate thin film strength with the nanoindentation technique, a three-dimensional pile-up analysis was proposed for an accurate determination of a closed two-dimensional boundary for the indentation-induced plastic zone. Leveling for the reference basal plane was done by extracting the surface height corresponding to zero net volume. The plastic zone boundary was determined from the outermost contour of the indented surface projected on the reference plane and then converted to effective radius of the hemispherical plastic zone. Nanoindentation marks on Au and TiN thin films are analyzed by applying this procedure. Yield strengths of Au and TiN thin films were estimated as 0.58 ± 0.04 and 11.07 ± 0.62 GPa, respectively. The data for TiN thin film was valuable because yield strength of this material cannot be estimated with the microtensile test due to brittle fracture before yielding. However, the yield strength of Au film was about two times higher than that of the microtensile test. This discrepancy was explained from the plastic flow blocked by a hard Si substrate. Due to the substrate, the expected hemispherical plastic zone was assumed to be changed into a disk shape. By modifying load-supporting area of the disk-shaped plastic zone, the recalculated yield strength of Au film was comparable to the microtensile result.

Acknowledgement

This research was supported by a grant from Center for Nanoscale Mechatronics & Manufacturing, one of the 21st Century Frontier Research Programs, which are supported by Ministry of Science and Technology, Korea.

References

- [1] W.C. Oliver and G.M. Pharr: *J. Mater. Res.* Vol. 7 (1992), p. 1564.
- [2] Y.-H. Lee and D. Kwon: *Key Eng. Mater.* Vols. 161-163 (1999), p. 569.
- [3] J.-H. Ahn, E.-c. Jeon, Y. Choi, Y.-H. Lee and D. Kwon: *Cur. Appl. Phys.* Vol. 2 (2002), p. 525.
- [4] Y.-H. Lee and D. Kwon: *J. Mater. Res.* Vol. 17 (2002), p. 901.
- [5] D. Kramer, H. Huang, M. Kriese, J. Robach, J. Nelson, A. Wright, D. Bahr and W.W. Gerberich: *Acta Mater.* Vol. 47 (1999), p. 333.
- [6] K.L. Johnson: *Contact Mechanics* (Cambridge University Press, U.K. 1985).
- [7] Y.-H. Huh, D.-I. Kim, J.-H. Hahn, G.-S. Kim, C.-D. Kee, S.-C. Yeon and Y.H. Kim: *Mater. Res. Soc. Symp. Proc.* Vol. 875 (2005), p. O4.15.1.